Synthesis and Magnetic and Transport Properties of $Sr_6V_9S_{22}O_2$: "AM_2S_5" Phases Revisited

J. B. Litteer,[1a] B.-H. Chen,[1a,c] James C. Fettinger,[1a] B. W. Eichhorn,*[,1a] H. L. Ju,[1b] and R. L. Greene[1b]

Center for Superconductivity Research, Departments of Chemistry and Physics, University of Maryland, College Park, Maryland 20742

Received March 31, 1999

The compound $Sr_6V_9S_{22}O_2$ was prepared from SrS, sulfur, vanadium metal, and V_2O_5 at 950 °C in an evacuated quartz tube. The compound is rhombohedral, $R\bar{3}$, with $a = 8.7538(6)$ Å, $c = 34.934(3)$ Å, and $Z = 3$, and shows strong preferred orientation in its XRD profiles (00*l*) due to the layered nature of the structure. The compound contains charged CdI_2 type VS_2 layers of formula $[V_7S_{14}]^{4-}$ separated by $[Sr_6(VOS_3)_2(S_2)]^{4+}$ layers. The latter has VOS_3^{3-} tetrahedra and S_2^{2-} disulfide units linked by Sr^{2+} ions. Magnetic susceptibility and four-probe resistivity studies show essentially temperature-independent paramagnetism above 80 K and small gap semiconductor behavior, respectively. The compound has a positive Hall coefficient at room temperature. The relationship among $Sr_6V_9S_{22}O_2$, "SrV_2S_5" (*J. Solid State Chem.* **1996**, *126*, 189), and other AM_2S_5 phases is discussed.

Introduction

Layered transition metal chalcogenides have been of interest for years because of their novel mechanical and electrical properties.[2−9] Of these, the intercalation compounds of the early transition metal MQ_2 phases (Q = S, Se) are the most well studied[4,10−15] due to their superconducting properties[16] at low temperatures. Structurally, this broad class of compounds is characterized by MQ_2 host layers that can accommodate a wide variety of guest intercalants (e.g. alkali-metal and alkaline-earth ions, organoamines, organometallics, etc.) into the interlayer van der Waals (VDW) gaps.[11] In most of these compounds, the periodicity of the intercalant is commensurate with the MQ_2 host. Intercalation of an AQ rock salt layer (A = rare earth) in the VDW gap of the MQ_2 compounds (M = group 4 or 5 metal) usually leads to $(AQ)_{1+x}(MQ_2)$ phases where $x \approx 0.1$. The AQ and MQ_2 layers in these compounds are alternately stacked along the *c*-axis of the cell but are incommensurate or "misfit" in the *a*−*b* plane.[17−20] More recently, a new type of misfit bilayer structure has been described[17,21−26] that can be viewed as a stage II analogue of the $(AQ)_{1+x}(MQ_2)$ phases. These $(AQ)_{1+x}(MQ_2)_2$ bilayer compounds are characterized by AQ rock salt layers inserted in every second VDW gap of the MQ_2 host. Structural investigations of $(LaS)_{1.14}(NbS_2)_2$ or "$LaNb_2S_5$" show two modifications with Nb partially occupying the "empty" VDW gaps in one of the modifications.[21,23−25]

Saeki and Onoda have prepared a similar series of compounds of empirical formula "AM_2S_5",[27−30] where A = alkaline earth and M = Nb and Ta. These phases are clearly layered (strong preferred 00*l* orientations in the XRD profiles), but despite the similarities in composition, they appear to differ structurally from the $(AQ)_{1+x}(MQ_2)_2$ type compounds just described. In addition, they reported that $SrNb_2S_5$ was superconducting at 3 K.[28] Unfortunately, the structures of these compounds are unknown. The Sr−V−S member of this series was originally characterized as a $Sr_2V_3S_7$ phase by our group[10,31] and subse-

(1) (a) University of Maryland, Chemistry. (b) University of Maryland, Physics. (c) Current Address: Lamont-Doherty Earth Observatory of Columbia University, Palisades, NY 10964.
(2) Rüdorff, W. *Angew. Chem.* **1959**, *71*, 487.
(3) Pell, M. A.; Vajenine, G. V. M.; Ibers, J. A. *J. Am. Chem. Soc.* **1997**, *119*, 5186.
(4) Schöllhorn, R. In *Inclusion Compounds*; Atwood, J. L., Davies, J. E. D., MacNicol, D. D., Eds.; Academic Press: London, 1984; Vol. I, p 249.
(5) Gamble, F. R.; Osiecki, J. H.; Cais, M.; Pisharody, R.; DiSalvo, F. J.; Geballe, T. H. *Science* **1971**, *174*, 493.
(6) Snyder, J. G.; Gelabert, M. C.; DiSalvo, F. J. *J. Solid State Chem.* **1994**, *113*, 355.
(7) Wiegers, G. A. *Jpn. J. Appl. Phys.* **1993**, *32*, 705.
(8) Mayer, J. M.; Schneemeyer, L. F.; Siegrist, T.; Waszczk, J. V.; Dover, B. V. *Angew. Chem., Int. Ed. Engl.* **1993**, *31*, 1645.
(9) Ramirez, A. P.; Cava, R. J.; Krajewski, J. *Nature* **1997**, *386*, 156.
(10) Eichhorn, B. W. In *Progress in Inorganic Chemistry*; Karlin, K. D., Ed.; John Wiley & Sons: New York, 1994; Vol. 42, p 139.
(11) Whittingham, M. S. *Prog. Solid State Chem.* **1978**, *12*, 41.
(12) Jacobson, A. J. In *Solid State Chemistry Compounds*; Cheetham, A., Day, P., Eds.; Oxford University Press: New York, 1992; p 182.
(13) Gamble, F. R.; Geballe, T. H. In *Treatise on Solid State Chemistry*; Hannay, N. B., Ed.; Plenum Press: New York, 1976; Vol. 3.
(14) Hullinger, F. In *Structural Chemistry of Layer-Type Phases*; Levy, F., Ed.; Reidel: Dordrecht, The Netherlands, 1976.
(15) *Intercalation Chemistry*; Academic Press: New York, 1982.
(16) Schöllhorn, R. In *Physics of Intercalation Compounds*; Pietronero, L., Tosatti, E., Eds.; Springer-Verlag: Berlin, New York, 1983; p 33.
(17) *Incomensurate Sandwiched Layered Compounds*; Meerschaut, A., Ed.; Trans. Tech. Publishers: Zurich, 1992; Vol. 100−101.
(18) Kato, V. K.; Kawada, I. *Acta Crystallogr.* **1977**, *B33*, 3437.
(19) Otero-Diaz, L.; FitzGerald, J. D.; Williams, T. B.; Hyde, B. G. *Acta Crystallogr.* **1985**, *B41*, 405.
(20) Takahashi, T.; Oka, T.; Yamada, O.; Ametani, K. *Mater. Res. Bull.* **1971**, *6*, 173.
(21) Meerschaut, A.; Guemas, L.; Auriel, C.; Rouxel, J. *Eur. J. Solid State Inorg. Chem.* **1990**, *27*, 557.
(22) Meerschaut, A.; Auriel, C.; Rouxel, J. *J. Alloys Compd.* **1992**, *183*, 129.
(23) Guemas, L.; Rabu, P.; Meerschaut, A.; Rouxel, J. *Mater. Res. Bull.* **1988**, *23*, 1061.
(24) Meerschaut, A.; David, T.; Moelo, Y.; Rouxel, J. *Eur. J. Solid State Inorg. Chem.* **1996**, *33*, 551.
(25) Meerschaut, A.; Roesky, R.; LaFond, A.; Deudon, C.; Rouxel, J. *J. Alloys Compd.* **1995**, *219*, 157.
(26) Roesky, R.; Meerschaut, A.; Rouxel, J.; Chen, J. *Z. Anorg. Allg. Chem.* **1993**, *619*, 117.
(27) Saeki, M.; Nozaki, H.; Onoda, M. *Mater. Res. Bull.* **1989**, *24*, 851.
(28) Saeki, M.; Onoda, M.; Ohta, M. *Mater. Res. Bull.* **1993**, *28*, 279.
(29) Saeki, M.; Onoda, M. *Trends Inorg. Chem.* **1991**, *1*, 1.
(30) Matsuura, K.; Wada, T.; Nakamizo, T.; Yamauchi, H.; Tanaka, S. *J. Solid State Chem.* **1991**, *94*, 294.

10.1021/ic990356f CCC: $19.00
Published on Web 01/07/2000

quently reported as SrV_2S_5 by Kijima et al.[32] The synthetic methods used by both groups involved reactions of SrS, vanadium metal, and elemental sulfur at 700−950 °C in evacuated quartz tubes. We report here that the true identity of this compound is $Sr_6V_9S_{22}O_2$ which contains an oxythiovanadate unit, VOS_3^{3-}, and a disulfide group. The relationship of this compound to the other AM_2S_5 phases is also discussed.

Experimental Section

Sample Preparation. Method A. The precursors (Cerac) SrS (99.9%), V (99.5%), V_2O_5 (99.9%), and S (99.999%) in a 2:2.73:0.134:5.33 ratio were intimately ground, loaded into a silica ampule, and sealed under vacuum. The contents were heated to 950 °C at 1.0 °C/min and calcined at 950 °C for 5 days. The samples were subsequently oven cooled (0.2 °C/min) yielding a black crystalline product. The reaction did not result in the devitrification of the silica ampule. XRD analysis of the product showed only the title compound.

Method B. The precursors SrS, V, and S in a 2:3:6 ratio were intimately ground, loaded into a silica ampule, sealed under vacuum, and heated as described in method A above. The reaction did not result in the devitrification of the silica ampule. The source of oxygen is not known. The product contained small amounts of SrS which were washed out of the samples by extracting with cold water.

H_2S Reaction. Black, single-phase $Sr_6V_9S_{22}O_2$ was loaded into an alumina crucible and placed in a flow-through reactor in a tube furnace. The sample was heated to 950 °C for 3 h in a flowing H_2S atmosphere. The resulting product was black and microcrystalline.

Sample Characterization. Powdered samples were characterized by powder X-ray diffraction (XRD) using a Rigaku DMAX-B diffractometer (Cu Kα radiation) and MDI data analysis package. Energy-dispersive X-ray analysis (EDX) was performed on a JEOL JXA-840 A electron probe microanalyzer. IR spectra were measured using a Nicolet Magna 560 infrared spectrometer equipped with a horizontal diffuse reflectance Gemini attachment. After data collection, the spectra were corrected for optical dispersion. Atomic absorption analysis was performed by Desert Analytics, Tucson, AZ. Samples for analysis were prepared as described above. Anal. Calcd for $Sr_6V_9S_{22}O_2$ (method B): Sr, 30.6; V, 26.6. Found: Sr, 31.3; V, 26.6.

Property Measurements. Dc magnetic susceptibility was measured between room temperature and 2 K using a SQUID magnetometer (Quantum Design model MPMS). Electrical resistivity as a function of temperature was measured by employing a standard ac method (~100 Hz) on bar-shaped sintered ceramic samples. Electrical contacts were made with silver paste.

X-ray Crystallography. A black plate with approximate dimensions $0.145 \times 0.127 \times 0.044$ mm^3 was placed and optically centered on the Bruker SMART1000 single-crystal CCD diffractometer. The crystals' initial unit cell parameters and crystal orientation matrix were determined from a least-squares analysis of a random set of reflections collected via three sets (30 frames/set) of 0.3° wide scans that were well distributed in reciprocal space. The intensity data were collected with 0.3° wide scans (40 s/fram) and a crystal to detector distance of 4.97 cm thus providing a complete sphere of data to 55° in 2θ. The unit cell was optimized using all of the frames from the initial series (606 frames) and a random set of frames chosen from the subsequent data collection runs and used throughout the data reduction sequence. A total of 8442 data ($\pm h \pm k \pm l$) were corrected for Lorentz and polarization effects using the SAINT+ data reduction program with 1188 unique [R(int) = 0.0591]. An empirical absorption correction was applied to the data based upon equivalent reflection measurements using Blessing's method in the program SADABS.

Systematic absences clearly indicated the centrosymmetric rhombohedral space group $R\bar{3}$ (No. 148), and the SHELXTL[33] program package was implemented to confirm the space group choice, to apply the absorption correction, and to set up the initial files. The structure was determined by direct methods with the successful location of the Sr and V atoms using the program XS[34] and refined with XL.[35] The remaining atoms were located from two subsequent difference Fourier maps. After several cycles of refinement, all of the atoms, except for the oxygen atom, were refined anisotropically. The final structure was refined to convergence [$\Delta/\sigma \leq 0.001$] with $R(F) = 4.37\%$, $wR(F^2) = 11.18\%$, and GOF = 1.099 for all 1188 unique reflections [$R(F) = 4.08\%$ and $wR(F^2) = 11.05\%$ for those 1080 data with $F_o > 4\sigma(F_o)$]. A final difference Fourier map possessed several peaks as large as $|\Delta\rho| \leq 3.23$ e Å^{-3}.

Several crystals (>15) were mounted and analyzed in the course of the crystallographic investigation; however, we were only able to index three of the crystals despite the strong diffraction from all samples. Axial photographs indicated that most crystals were not single although their optical appearance looked quite regular.

Results

Synthesis and Characterization. The optimal synthetic conditions for the preparation of $Sr_6V_9S_{22}O_2$ involves SrS and V_2O_5 with elemental V and S heated at 800−950 °C in stoichiometric proportions. Single heat treatments of these reagents give single-phase product without regrinding or reheating. The resulting black platelike crystals show a high degree of preferred orientation as evidenced by the dominant 00*l* reflections in the XRD profile (Figure 1). Essentially single-phase product was also obtained in the presence of excess sulfur without the use of V_2O_5 in the synthesis mixture. However, the resulting product is less crystalline when an oxide source is not used in the synthesis and small amounts of SrS and S_8 impurities remained after heating. The source of oxygen from this method is unknown. The excess SrS in the product was removed by washing the samples with water and the excess S_8 sublimed to the cold end of the tube. Elemental analyses of the crystals from this preparative method are in excellent agreement with the calculated composition from the X-ray structure determination. Qualitative EDX analyses of the crystals were also consistent with the X-ray composition. The IR diffuse reflectance spectrum is essentially featureless showing a single weak absorbance at 775 cm^{-1}. We assign this band as the V−O stretch due to the similarities in energy with other vanadyl compounds.[36,37]

$Sr_6V_9S_{22}O_2$ is unchanged by annealing under vacuum at 1050 °C for 18 h. However, reaction of the compound with flowing H_2S at 950 °C for 3 h results in the extrusion of SrS and the formation of a new unidentified phase. Analysis and property measurements on the phase are currently under investigation.

Structure. $Sr_6V_9S_{22}O_2$ is rhombohedral, space group $R\bar{3}$, with $a = 8.7538(6)$ Å and $c = 34.934(3)$ Å. A summary of the crystallographic data is given in Table 1. A listing of the fractional coordinates is given in Table 2, and selected bond distances and angles are found in Table 3. The phase can be described as an oxysulfide intercalation compound of VS_2 resulting in a $[V_7S_{14}]^{4-}$ host layer separated by a $[Sr_6(VOS_3)_2(S_2)]^{4+}$ guest layer (see Figure 2a). The $[V_7S_{14}]^{4-}$ layer has a typical CdI_2 type structure[38] defined by a two-dimensional array of edge-shared $VS_{6/3}$ octahedra (Figure 2b). On the basis of charge considerations of the $[Sr_6(VOS_3)_2(S_2)]^{4+}$ guest layer (see

(31) Eichhorn, B. W.; Chen, B.-H. Original manuscript was not published due to problems with reproducibility. See ref 196 in ref 10 above.
(32) Kijima, N.; Ikeda, S.; Shimono, I.; Matsumoto, T.; Tsuji, S.; Kumagai, K.; Nagata, S. *J. Solid State Chem.* **1996**, *126*, 189.
(33) Sheldrick, G. M. *SHELXTL;* Siemens Analytical X-ray Instruments, Inc.: Madison, WI, 1994.
(34) Sheldrick, G. M. *Acta Crystallogr.* **1990**, *A46*, 467.
(35) Sheldrick, G. M. *XL refinement program;* University of Gottingen: Gottingen, Germany, 1993.
(36) Asgedom, G.; Sreedhara, A.; Kivikoski, J.; Valkonen, J.; Rao, C. P. *J. Chem. Soc. Dalton Trans.* **1995**, 2459.
(37) Ligtenbarg, A. B. J.; Spek, A. L.; Hage, R.; Feringa, B. L. *J. Chem. Soc., Dalton Trans.* **1999**, 659.
(38) Onoda, M.; Kato, K. *Acta Crystallogr.* **1990**, *B46*, 487.

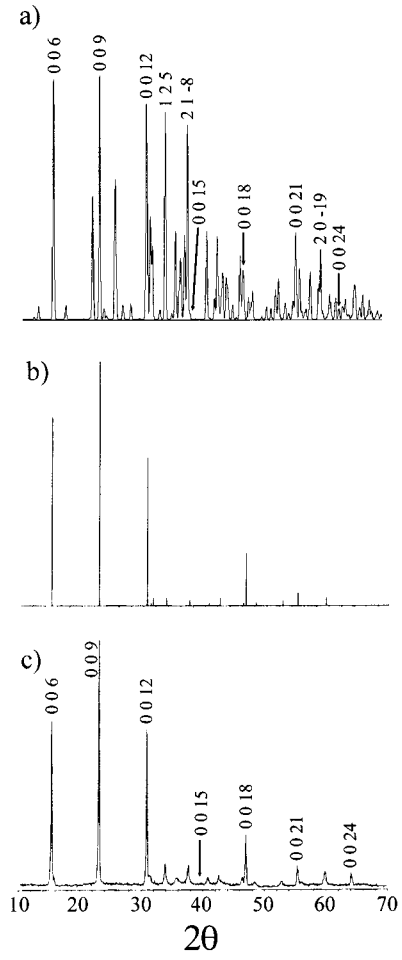

Figure 1. Calculated (a) and observed (c) XRD profiles (Cu Kα radiation) for $Sr_6V_9S_{22}O_2$ showing the Miller indices of selected peaks. The preferred orientation of the sample is evidenced by the strong 00*l* reflections in the observed pattern. The XRD data for SrV_2S_5 from ref 32 are represented by the stick pattern (b).

Table 1. Crystal Data for $Sr_6V_9S_{22}O_2$

fw	1721.50
temp	153(2) K
wavelength	0.710 73 Å
space group	$R\bar{3}$
unit cell dimens	$a = 8.7538(6)$ Å
	$c = 34.934(3)$ Å
V	2318.3(3) Å^3
Z	3
D (calcd)	3.699 g/cm^3
abs coeff	14.334 mm^{-1}
final R indices [$I > 2\sigma(I)$][a]	R1 = 0.0408, wR2 = 0.1105
R indices (all data)[a]	R1 = 0.0437, wR2 = 0.1118

[a] $R1 = \sum|F_o - F_c|/\sum F_o$; $wR2 = (\sum w|(F_o)^2 - (F_c)^2|^2/\sum wF_o^2)^{1/2}$.

below), the VS_2 host layer appears to be negatively charged with an average vanadium oxidation state of +3.43 (i.e. $[V_7S_{14}]^{4-}$). The 3.31 Å VS_2 subcell is denoted by the dotted lines in Figure 2b whereas the actual unit cell is indicated by bolded lines. The observed *a* lattice constant is $\sqrt{7}$ times larger than the subcell due to the larger repeat unit mandated by the interleaving $[Sr_6(VOS_3)_2(S_2)]^{4+}$ layer. As a result, there are two crystallographically distinct vanadium atoms in the $[V_7S_{14}]^{4-}$ layer, V(1) and V(2). The V−S bond distances involving V(2) are 2.366(1) Å whereas the those to V(1) are 2.39(2) Å (averages). These distances are quite similar to the V−S contacts in $(PbS)_{1.2}VS_2$, which are in the range 2.37(2)−2.39(2) Å.[38]

Table 2. Atomic Coordinates ($\times 10^4$) and Equivalent Isotropic Displacement Parameters (Å^2 $\times$ 10^3) for $Sr_6V_9S_{22}O_2$

	x	*y*	*z*	*U*(eq),[a] Å^2
Sr(1)	9775(1)	3826(1)	1117(1)	10(1)
V(1)	8534(1)	2875(1)	−7(1)	13(1)
V(2)	0	0	0	15(1)
V(3)	0	0	1530(1)	5(1)
S(1)	471(1)	2380(1)	400(1)	4(1)
S(2)	9029(1)	5253(1)	408(1)	3(1)
S(3)	6667	3333	−431(1)	5(1)
S(4)	132(2)	7740(2)	334(1)	8(1)
S(5)	3333	6667	366(1)	16(1)
O(1)	0	0	2023(2)	8(1)

[a] *U*(eq) is defined as one-third of the trace of the orthogonalized $\mathbf{U}_{ij}$ tensor.

Table 3. Bond Lengths (Å) and Angles (deg) for $Sr_6V_9S_{22}O_2$

Sr(1)−O(1)	2.622(2)	V(1)−S(1)	2.377(1)
Sr(1)−S(5)	2.983(1)	V(1)−S(3)	2.385(2)
Sr(1)−S(2)	2.987(2)	V(1)−S(2)	2.389(1)
Sr(1)−S(1)	3.002(1)	V(1)−S(2)	2.392(1)
Sr(1)−S(4)	3.100(1)	V(1)−S(1)	2.411(1)
Sr(1)−S(4)	3.101(1)	V(2)−S(1)	2.366(1)
Sr(1)−S(4)	3.130(1)	V(3)−O(1)	1.724(6)
Sr(1)−S(4)	3.368(1)	V(3)−S(4)	2.150(1)
V(1)−S(2)	2.367(1)	S(5)−S(5)′	2.103(5)
O(1)−Sr(1)−S(5)	128.8(1)	S(2)−V(1)−S(3)	94.77(5)
O(1)−Sr(1)−S(2)	81.7(1)	S(1)−V(1)−S(3)	88.15(5)
S(5)−Sr(1)−S(2)	104.39(5)	S(2)−V(1)−S(2)′	87.74(6)
S(5)−Sr(1)−S(1)	104.33(5)	S(3)−V(1)−S(2)	94.13(5)
S(2)−Sr(1)−S(1)	67.55(3)	S(3)−V(1)−S(2)	88.37(5)
S(5)−Sr(1)−S(4)	67.31(3)	S(2)−V(1)−S(2)′	92.75(5)
S(2)−Sr(1)−S(4)	135.79(4)	S(1)−V(2)−S(1)	88.75(4)
S(1)−Sr(1)−S(4)	72.73(3)	S(1)−V(2)−S(1)	91.25(4)
S(5)−Sr(1)−S(4)	131.35(4)	O(1)−V(3)−S(4)	108.49(5)
S(2)−Sr(1)−S(4)	122.08(4)	S(4)−V(3)−S(4)	110.43(5)
S(2)−V(1)−S(1)	91.50(5)		

The $[Sr_6(VOS_3)_2(S_2)]^{4+}$ layer comprises two distinct structural entities, namely, VOS_3^{3-} tetrahedra and S_2^{2-} disulfide groups. An (001) projection of this layer is given in Figure 2c. The VOS_3^{3-} tetrahedron (Figure 3a) has V(3)−O1 and V(3)−S(4) contacts of 1.724(6) and 2.150(1) Å, respectively. The distances are very similar to those in the VOS_3^{3-} tetrahedra in the V^{5+} compound $Ba_6V_4O_5S_{11}$.[39] Due to these similarities, we assign a +5 oxidation state to V(3). The disulfide ligand has an S−S separation of 2.103(5) Å, which is typical for transition metal disulfides such as the pyrites and marcasites.[40] The Sr^{2+} ions link the VOS_3^{3-} tetrahedra and the disulfides together into a two-dimensional array. The Sr^{2+} ions are in seven coordinate monocapped trigonal prismatic environments as shown in Figure 3b. Each strontium ion shares an O−S and an S−S edge with two different VOS_3^{3-} tetrahedra and is bonded to two sulfides from the $[V_7S_{14}]^{4-}$ layer. In addition, there is a disulfide bound in an η^1 fashion to each Sr^{2+}. Each disulfide is connected to six Sr^{2+} ions (three to each sulfur) as shown in Figure 3c.

The long 34.934(3) Å *c*-axis results from the A−B−C alternation of the $[Sr_6(VOS_3)_2(S_2)]^{4+}$ layers. Each successive layer is shifted by $^1/_3$ along the 110 direction (see Figure 2a). The three different orientations leave different groups at the edges of the unit cell. The vanadyl groups are on the edges with the V−O "up" in layer A, the disulfides reside on the edges in B, and the vanadyls with V−O "down" are found in C. The repeat unit in the *a*−*b* plane of the $[Sr_6(VOS_3)_2(S_2)]^{4+}$ layer is

(39) Litteer, J. B.; Fettinger, J. C.; Eichhorn, B. W. *Acta Crystallogr.* **1997**, *C53*, 163.
(40) Wells, A. F. *Structural Inorganic Chemistry*, 5th ed.; Oxford University Press: New York, 1984.

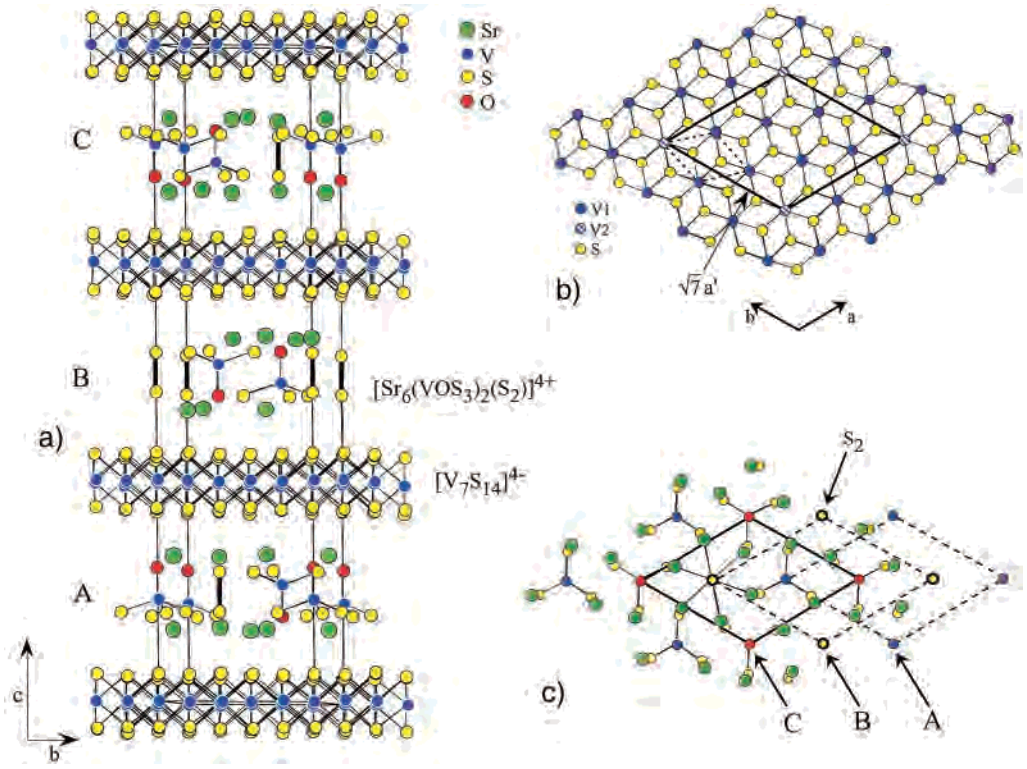

Figure 2. (a) Ball-and-stick drawing of the $Sr_6V_9S_{22}O_2$ structure showing the A−B−C alternation of the intercalation layers. The bold lines represent the unit cell. (b) 001 projection of the $[V_7S_{14}]^{4-}$ layer. The dashed lines represent the VS_2 subcell, and the bold lines represent the observed unit cell. (c) 001 projection of the $[Sr_6(VOS_3)_2(S_2)]^{4+}$ layer showing the A orientation.

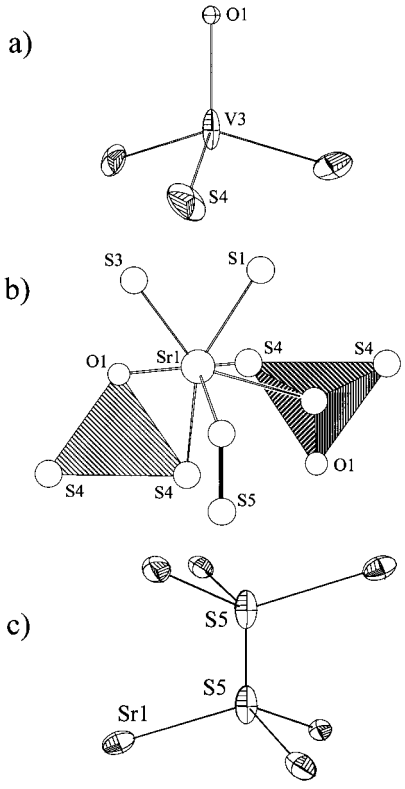

Figure 3. ORTEP drawings of (a) the VOS_3^{3-} tetrahedron, (b) the $SrOS_6$ polyhedron, and (c) the Sr_6S_2 unit in the $[Sr_6(VOS_3)_2(S_2)]^{4+}$ layer.

$\sqrt{7}$ times larger than the VS_2 subcell and is responsible for the 8.7538(6) Å *a* lattice parameter.

Transport and Magnetic Properties. Figure 4 shows the typical electrical resistivity of $Sr_6V_9S_{22}O_2$ as a function of temperature. The resistivity increases with decreasing temperature but the plot of log(ρ) vs T^{-1} does not indicate a constant semiconductor-like gap. Instead the slope of log(ρ) vs T^{-1} changes continuously with temperature but is suggestive of a small gap (<100 meV). For the temperature range between 4.2 and 20 K we find that our data are best fit to the expression for three-dimensional variable range hopping $\rho = \rho_0 \exp(T_0/T)^{1/4}$ with $T_0 = 4.1 \times 10^4$ K.

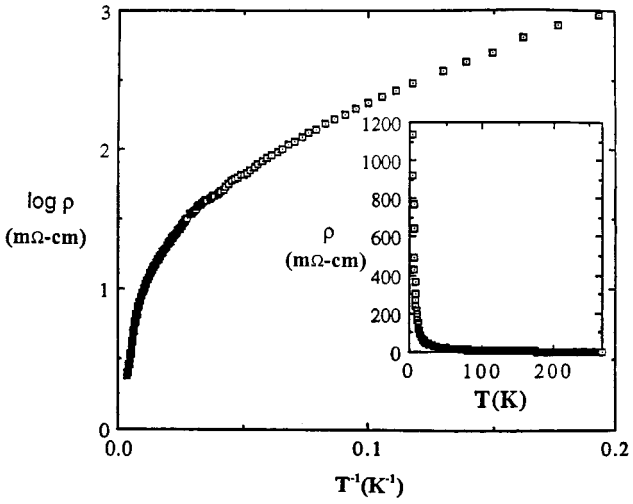

Figure 4. Plot of log(ρ) vs T^{-1} for $Sr_6V_9S_{22}O_2$.

Figure 5 shows the magnetic susceptibility of $Sr_6V_9S_{22}O_2$ as a function of temperature. The susceptibility does not vary significantly in the temperature range between 40 and 300 K. Between 200 and 300 K, the susceptibility is nearly constant and exhibits a minimum value near 100 K. Curie−Weiss behavior is observed below 100 K. The data below 100 K can be fit to $\chi = \chi^0 + C/(T - \Theta)$, where χ^0 is the temperature-independent susceptibility, Θ is the Weiss temperature, and C is the Curie constant. The constants χ^0, Θ, and C are determined

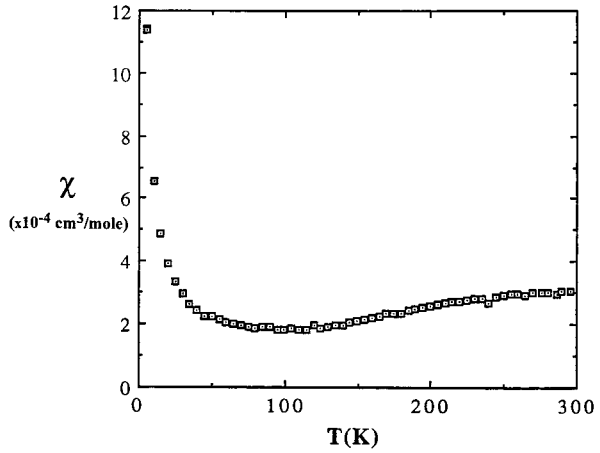

Figure 5. Plot of χ vs T for $Sr_6V_9S_{22}O_2$.

by a least-squares fit: $\chi^0 = 1.0 \times 10^{-4}$ (cm^3/mol), $\Theta = 1.0$ K, and $C = 6.1 \times 10^{-3}$ ((cm^3 K)/mol). The magnitude of the Curie constant suggests that the temperature-dependent component of the susceptibility may be due to ferromagnetic impurities. The Hall coefficient at 300 K is positive with $R_H = 2.5 \times 10^{-3}$ cm^3/C.

Discussion

The $Sr_6V_9S_{22}O_2$ phase represents a new type of mixed-metal intercalation compound. It is similar in composition to stage II $(AS)_{1+x}(MS_2)_2$ bilayer phases of Nb and Ta;[24,41] however, $Sr_6V_9S_{22}O_2$ is a stage I compound with VOS_3^{3-} and S_2^{2-} groups intercalated into the VS_2 host. It is a small gap semiconductor and shows essentially temperature-independent paramagnetism with $\chi^0 = 1.0 \times 10^{-4}$ cm^3/mol. Given the layered nature of the structure (cf. the copper oxides) and the temperature-independent nature of the susceptibility may indicate the compound is a Heisenberg or XY antiferromagnet.[42] Additional experiments, such as neutron scattering, are needed to address this issue.

The $Sr_6V_9S_{22}O_2$ phase reported here is clearly the true identity of the "$Sr_2V_3S_7$" and "SrV_2S_5" phases previously reported.[10,32] This conclusion is based on the following observations: (1) The XRD profiles of the three phases (Figure 1) are identical and show the same preferred orientation.[32] (2) The electron diffraction patterns of SrV_2S_5 give a 3.314 Å $\times$ 35.023 Å cell with an unusual $\sqrt{7}$ superstructure[32] that is identical to that of $Sr_6V_9S_{22}O_2$ (Figure 2). (3) $Sr_6V_9S_{22}O_2$ reacts with H_2S to give a new compound suggesting that only the *oxy*sulfide can adopt the 35 Å structure. (4) The magnetic data for SrV_2S_5 and $Sr_6V_9S_{22}O_2$ are the same.[32] The Nb analogue appears to be quite similar to $Sr_6V_9S_{22}O_2$ (by XRD) and is currently under investigation.

Acknowledgment. We thank the NSF-DMR 9223060 and EPRI for financial support of this work.

Supporting Information Available: Text describing complete crystallographic experimental details and tables listing detailed crystallograpic data, atomic positional parameters, anisotropic thermal parameters, and bond lengths and angles. This material is available free of charge via the Internet at http://pubs.acs.org.

IC990356F

(41) Roesky, R.; Meerschaut, A.; Vanderlee, A.; Rouxel, J. *Mater. Res. Bull.* **1994**, *29*, 1149.
(42) Chakravarty, S.; Halperin, B. I.; Nelson, D. R. *Phys. Rev.* **1989**, *B39*, 2344.